

Interaction between turbulence and a nonlinear tearing mode in the low β regime

F. Militello, F. L. Waelbroeck, R. Fitzpatrick, and W. Horton

Institute for Fusion Studies, The University of Texas at Austin, Austin, Texas 78712, USA

(Received 16 January 2008; accepted 7 April 2008; published online 22 May 2008)

The interaction between turbulence and a nonlinear tearing mode is investigated numerically using a 2D electrostatic model. Turbulence is found to cause transitions between the different roots for the propagation velocity of the mode. The transitions take the mode towards roots with slower propagation that are characterized by a locally flattened density profile. For sufficiently large islands the transition reduces the drive for the tearing mode. © 2008 American Institute of Physics.

[DOI: 10.1063/1.2917915]

The nonlinear evolution of the tearing mode is of interest in many contexts. In the magnetotail^{1,2} and the solar corona,³ the nonlinear tearing mode may be viewed as a model for the predisruptive evolution of plasmoids and flux ropes. In tokamaks, the neoclassical tearing mode gives rise to magnetic islands that degrade confinement.⁴ In stellarators, by contrast, externally controlled magnetic islands are used as divertors to control edge transport and improve confinement.⁵

Theoretical investigations of the nonlinear tearing mode have often relied on the assumption that plasma turbulence can be modeled by using anomalous transport coefficients. In many cases of interest, however, the characteristic size of turbulent eddies is comparable to the width of the magnetic island so that this assumption is questionable.⁶ Furthermore, magnetic islands are known to locally flatten the temperature and density gradients that provide the drive for the turbulence.^{7,8} Investigations of the effects of turbulence on tearing modes found that the turbulence causes a diffusive broadening of the current channel⁹ and gives rise to negative viscosity and to the growth of zonal flows.^{10–13} For a nonlinear tearing mode, such zonal flows will affect mode growth through the polarization current.¹⁴

In the present paper we examine self-consistently the mutual interaction of an island with turbulence. Our analysis exploits the fact that for an ordinary nonlinear tearing mode,^{15,16} the growth rate $\eta\Delta'/w$ is small compared to the characteristic frequency ω_* of the turbulent fluctuations. Here η is the resistivity, Δ' is the standard tearing mode stability parameter, w is the island width, and $\omega_* = v_* k_y$ is the diamagnetic frequency, k_y is the island poloidal wave number, and $v_* = cT_e/(eB_z L_n)$ (e is the electric charge, T_e is the constant electron temperature, c is the speed of light). In a frame moving with the island, the electromagnetic induction associated with the tearing mode is then negligible. The turbulent electromagnetic induction is also negligible whenever $\hat{\beta} = \beta L_s^2/L_n^2 \ll 1$, where β is the ratio of kinetic to magnetic pressures and L_n , L_s are the density and magnetic shear lengths, respectively.⁶ Under the stated conditions, the dynamics is thus approximately electrostatic in the island's frame. A distinguishing feature of our electrostatic simulations is that we allow the propagation velocity of the island to evolve dynamically, and we infer the growth or decay of

the nonlinear tearing mode from the spatial integral of the component of the current-density that is in phase with the island.

We carry out our investigation in a 2D slab configuration ($\partial_z = 0$). The magnetic field takes the form $\mathbf{B} = B_z \mathbf{e}_z + \mathbf{e}_z \times \nabla \psi$, where B_z is the guide field and the transverse flux ψ is taken to have the “constant- $\tilde{\psi}$ ” form¹⁵ $\psi = x^2/2 + \tilde{\psi} \cos y$. This magnetic field exhibits an island with full width $w = 4\tilde{\psi}^{1/2}$. We use the Hasegawa–Wakatani model¹⁷ consisting of the electron continuity equation describing the conservation of density, n , and an equation for the evolution of plasma vorticity, $U = \nabla^2 \varphi$,

$$\partial n / \partial t + \mathbf{v} \cdot \nabla n = C^{-1} \nabla_{\parallel}^2 (n - \varphi) + D \nabla^2 n, \quad (1)$$

$$\partial U / \partial t + \mathbf{v} \cdot \nabla U = C^{-1} \nabla_{\parallel}^2 (n - \varphi) + \mu \nabla^2 U, \quad (2)$$

where $\nabla_{\parallel} F = \mathbf{B} \cdot \nabla F$ and $\mathbf{v} = \mathbf{e}_z \times \nabla \varphi$. The time is normalized with respect to the drift-time ω_*^{-1} , the transverse coordinate x and y are normalized to ρ_s and k_y^{-1} , respectively, where $k_y \rho_s \ll 1$, \mathbf{B} is normalized to $\rho_s B_{y0}'$ where the prime denotes derivation with respect to x , the velocities to v_* , and the density to $\rho_s n_0'$. Here $\rho_s = c_s / \omega_{ci}$, where $c_s = \sqrt{T_e / m_i}$ is the ion-sound speed and ω_{ci} is the ion cyclotron frequency. The time-scale separation argument presented above, together with the choice of a frame of reference moving with the island, justifies the neglect of the electromagnetic induction in Ohm's law. The parameters D and μ are the particle diffusion coefficient and the ion viscosity, respectively, and $C = c^2 \eta (8\pi)^{-1} \rho_s^{-2} \omega_*^{-1} \beta (L_s / L_n)^2$ is the normalized resistivity.

The model equations (1) and (2) have previously been used by Scott *et al.*⁷ to investigate resistive drift wave turbulence in the absence of an island ($w=0$). These authors have shown that the dynamics exhibits the following limiting behaviors. In the inner region, $k_{\parallel} \ll C^{1/2}$, collisional friction restricts parallel electron flow so that the electrons are essentially incompressible. In this region the turbulence is hydrodynamic in nature (i.e., described by the 2D Navier–Stokes model). In the outer region ($k_{\parallel} \gg C^{1/2}$), by contrast, resistivity plays a negligible role and parallel force balance

leads to a Boltzmann response of the density to electrostatic fluctuations, $\tilde{n} = \tilde{\phi}$. In the outer region Eqs. (1) and (2) reduce to the modified Hasegawa–Mima model.¹⁸

An important property of Eqs. (1) and (2) is that $\phi = n = x$ is an exact solution representing an island traveling at the electron diamagnetic velocity, i.e., an island at rest in the electron fluid. We will refer to this solution as the universal root since it is valid for arbitrary values of the parameters. Numerical simulations and analytic calculations assuming quiescent conditions show that there are other roots to the equilibrium problem.^{8,19}

We complete Eqs. (1) and (2) with the following boundary conditions. We keep the density at the edge fixed, $n(\pm l_x) = \pm l_x$, and require the vorticity to vanish, $U(\pm l_x) = 0$. For $k_y \rho_s \ll 1$, the latter condition approximates the requirement that the diffusive momentum flux through the edge vanish, $U \approx \partial_x^2 \phi = v_y'(\pm l_x) \approx 0$, corresponding to a freely propagating island. Lastly, we fix the electrostatic potential at the edge according to $\phi(\pm l_x) = \mp u l_x$, where u is the phase velocity of the island in the frame where the background electric field vanishes. This boundary condition approximates the condition $v_y(l_x) = \partial_x \phi(l_x) = -u$ provided that $w \ll l_x$. Note that the minus sign reflects the fact that in the frame moving with the island the plasma flow is opposite to the direction of the island in the frame where the plasma is at rest.

The choice of boundary conditions raises the question of how to determine the phase velocity u of the nonlinear tearing mode. To answer this question, consider the azimuthal (\hat{e}_y) component of the momentum balance equation,

$$(\partial_t + \mathbf{v} \cdot \nabla) v_y = -\partial_y n - J \tilde{\psi} \sin y + \mu \nabla^2 v_y,$$

where $v_y = \partial_x \phi$ and $J = \nabla^2 \psi / \beta$ is the plasma current along \mathbf{e}_z . Integrating this equation over the simulation volume and using the boundary conditions described above, we find after some integrations by parts

$$\partial_t \mu = F_y(u, \tilde{\psi}), \quad (3)$$

where F_y is the azimuthal electromagnetic force acting on the fluid in the island region,

$$F_y(u, \tilde{\psi}) \equiv \frac{\tilde{\psi}}{4\pi l_x} \int_{-l_x}^{l_x} dx \int_{-\pi}^{\pi} dy J(x, y; u, \tilde{\psi}) \sin y.$$

For consistency with our assumption of steady state, we must determine the island velocity so that $F_y(u, \tilde{\psi}) = 0$, a condition that indicates force balance.

In addition to driving zonal flows that contribute to the modification of the island propagation velocity, the turbulent fluctuations also drive parallel polarization currents that affect the island amplitude. Their effect on the evolution of w is governed by the “generalized Rutherford equation,”^{4,15}

$$\frac{0.823}{C} \frac{dw}{dt} = \Delta'(w) + \Delta_{\text{pol}}(u, w), \quad (4)$$

obtained by matching the perturbed magnetic field \tilde{B}_y at the boundary of the simulation domain. The left-hand side of this equation represents the small electromagnetic induction, re-

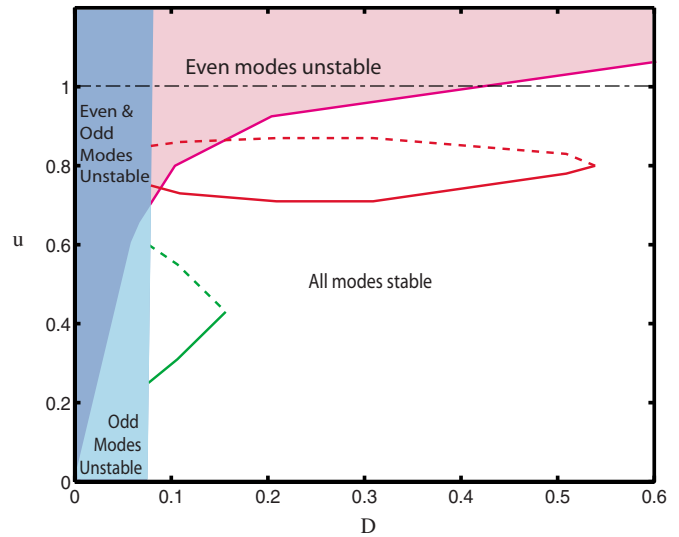


FIG. 1. (Color online) Stability diagram for the dissipative drift wave for $w = 2.9$. The shaded regions show the domains of instability for the even and odd dissipative drift waves and the lines show the phase velocity of the unforced ($F_y = 0$) island as a function of $D = \mu$ when parity is enforced. Unstable roots are represented with dashed lines.

tained here in order to describe the island evolution. The first term on the right-hand side represents the drive from currents flowing outside the island region, while the second term, $\Delta_{\text{pol}}(u, w)$, measures the effects of the internal polarization current, including that generated by the turbulence. This term takes the form

$$\Delta_{\text{pol}}(u, w) \equiv -\frac{1}{\pi \tilde{\psi}} \int_{-l_x}^{l_x} dx \int_{-\pi}^{\pi} dy (J - \langle J \rangle_{\psi}) \cos y, \quad (5)$$

where $\langle \cdot \rangle_{\psi}$ represents the average across an infinitesimal tube of flux ψ . In summary, we quantify the effect of the turbulence on island propagation in terms of the azimuthal force F_y and its effect on island size in terms of the matching parameter Δ_{pol} .

Self-sustained turbulence requires a sufficiently large number of linearly unstable modes. In the present model, the resistive drift-waves are driven unstable by the density gradient. Experiments and simulations have shown, however, that magnetic islands flatten the density gradients for a broad range of conditions.^{8,20} In order to guide the choice of parameters for the nonlinear simulations, we have used a linear eigenvalue code (benchmarked with analytical results^{21,22}) to investigate the linear stability properties. To model the effects of density flattening we have used the equilibrium density profile $n'(x) = 1 - [1 - n'(0)] \exp(-x^2/w^2)$. Recall that due to the frozen-in property, electrons inside the separatrix must propagate at the same velocity as the island. Thus, the degree of flattening $n'(0)$ must be such that the island velocity matches the electron diamagnetic velocity inside the separatrix, $u \approx n'(0)$.

Figure 1 shows the marginal stability curves in the plane (u, D) for modes with even and odd parity about $x = 0$. Note that the marginal stability points in the absence of flattening lie at the intersection of the line $u = 1$ with the stability boundaries. Figure 1 shows that there is a region of param-

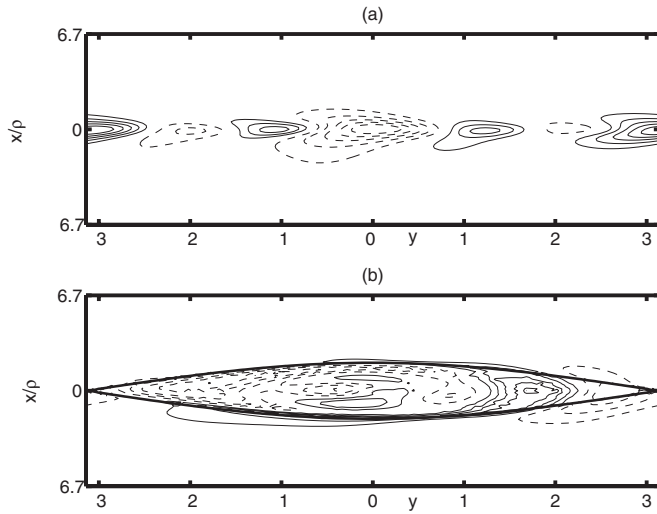


FIG. 2. Contour plot of $H = n - \phi - \langle n - \phi \rangle \psi$ (a) without and (b) with a magnetic island.

eter space where only even modes are unstable. Given the odd parity of the equilibrium, this region offers the opportunity to suppress numerically the turbulence by imposing an odd parity on the dynamics. Enforcing parity makes it possible to compare the turbulent and quiescent states for the same values of the parameters.

We have solved systems (1) and (2) using an initial-value, finite-difference code that uses a fully implicit algorithm.²³ The size of the numerical box is $l_x = 6.7$ and the grid resolution is 100×112 points. We initialize the simulations with randomly phased adiabatic perturbations described by the spectral distribution $|n_k| \propto k^2/(1+k^4)$. A Gaussian envelope localizes the seed perturbations in the central region of the numerical box with amplitudes in the linear regime.

The qualitative properties of the system are indicated in Fig. 2 by a comparison between the nonadiabatic component of the density, $H = n - \phi - \langle n - \phi \rangle \psi$ in a case (a) without, and (b) with an island. In the first case the nonadiabatic perturbations are concentrated in the hydrodynamic layer, as expected.⁷ In the presence of an island, by contrast, perturbations propagate along the field away from the hydrodynamic region, thereby spreading across the entire island.

In order to gain some understanding of the effects of turbulence on the island, we begin by investigating the response of the system to an island moving with a constant velocity. Figures 3 and 4 show F_y and Δ_{pol} as a function of the velocity, u , for two different island widths $w = 0.5$ and $w = 2.9$, and for $D = \mu = 0.1$ and $C = 1$. The solid lines represent cases where the odd parity of the fields is enforced, so that turbulence is suppressed, while the dashed lines represent time-averaged values of F_y and Δ_{pol} in simulations where both parities are allowed to evolve.

Of particular interest are the multiple unforced solutions described by the intersections of the force curve with the abscissa and marked by vertical lines in Figs. 3 and 4. For the value $C = 1$ used here the unforced solutions other than the universal root all correspond to $u < 1$ and thus to flattened density profiles. Note that the stability of any root with respect to a change in velocity can be determined from the

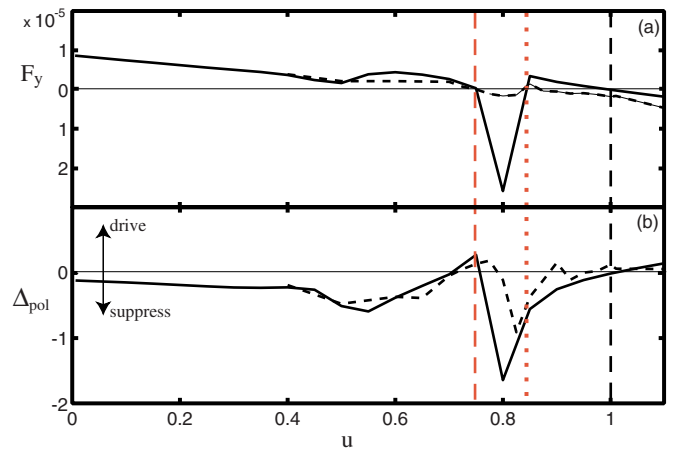


FIG. 3. (Color online) (a) Perpendicular force F_y acting on the island and (b) stability parameter Δ'_{pol} vs imposed velocity u for $w = 0.5$. The solid lines represent laminar states (parity enforced numerically) and the dashed lines are the time-averaged values in the turbulent states. The vertical dashed (dotted) lines indicate stable (unstable) unforced states.

derivative of the force with respect to the velocity, with $dF_y/du < 0$ and $dF_y/du > 0$ indicating that the root is, respectively, stable (dashed vertical lines) and unstable (dotted vertical lines) against small perturbations in u . Comparison of Fig. 3(a) with Fig. 4(a) shows that increasing w leads to the formation of new pair of stable/unstable roots at $u \approx \{0.35, 0.55\}$. Increasing the island width further leads to the merger and annihilation, at some width $2.9 < w < 4.1$, of the pair of roots at $u \approx \{0.55, 0.75\}$ in Fig. 4.

It is instructive to draw the locus of unforced ($F_y = 0$) solutions of the laminar nonlinear simulations in the linear stability diagram of Fig. 1. The solid and dashed lines in this diagram represent the velocity of the roots corresponding, respectively, to stable and unstable propagation for the case with enforced parity and for $w = 2.9$. These lines lie mostly in the regime where dissipative drift waves are stable, reflecting the stabilizing effect of density flattening. The two higher-velocity roots, however, cross the stability limit for even modes at $D \approx 0.16$ and $D = 0.09$. We thus expect turbulence to develop in these states when both parities are allowed to evolve.

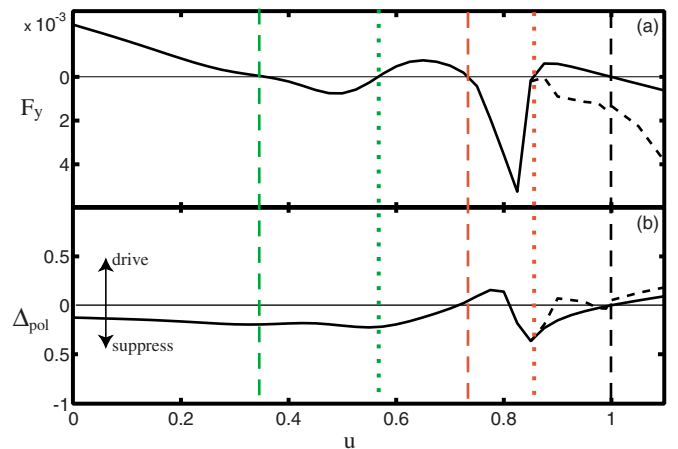


FIG. 4. (Color online) Same as Fig. 3 but for $w = 2.9$.

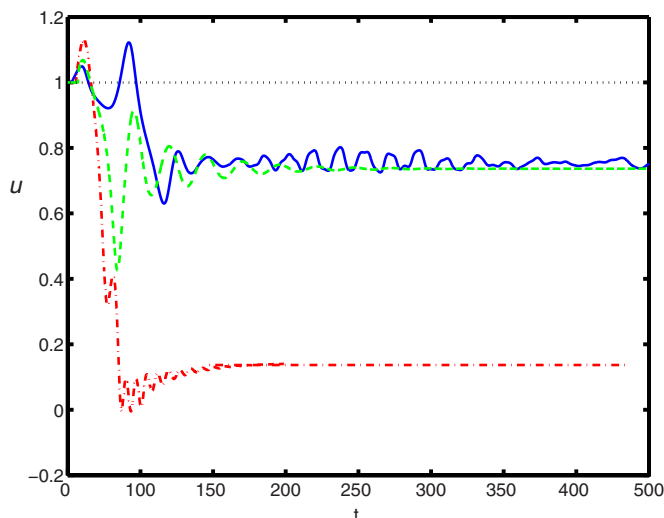


FIG. 5. (Color online) Time evolution of the phase velocity for $w=0.5$ (solid line), $w=2.9$ (dashed line), and $w=4.1$ (dashed-dotted line).

The predictions of the linear stability calculation in Fig. 1 are borne out by the dashed lines in Figs. 3 and 4 showing the dependence of the time average of F_y and Δ_{pol} on the velocity when both parities are allowed to evolve. When the linear stability condition described in Fig. 1 is violated, the dashed lines separate from the solid lines corresponding to the parity-enforced, quiescent simulation. The difference describes the effect of the turbulence on the island at fixed velocity. Figures 3(b) and 4(b) show that over most of the range of parameters resulting in turbulence, its effect at fixed velocity is to drive island growth. Inspection of the force curve, however, shows that turbulence changes $F_y(u, \tilde{\psi})$ qualitatively. In particular, the universal root disappears in the presence of turbulence. This suggests that the more dramatic effect of turbulence is to cause transitions by modifying the unforced states available to the island.

In order to investigate transitions in the propagation velocity of the tearing mode we have implemented the velocity evolution Eq. (3) by adjusting the boundary condition on φ every time step. Figure 5 shows the evolution of the propagation velocity for islands initialized with $u=1$. With enforced parity the propagation velocity remains fixed at $u=1$ (dotted line). When we allow the turbulent fluctuations to develop, by contrast, the propagation velocity slows down abruptly. For $w=0.5$ (solid line), the velocity settles in a turbulent steady-state around the root at $u \approx 0.75$. Figure 3(b) shows that $\Delta_{\text{pol}} > 0$ for that root so that the transition increases the drive for the nonlinear tearing mode. For $w=2.9$ (dashed line), the final propagation velocity is similar to that for $w=0.5$ but the density flattening now extends over the entire hydrodynamic region ($w > C^{1/2} = 1$) with the result

that the dissipative drift waves are stable and the final state is quiescent. Figure 4 shows that $\Delta_{\text{pol}} \approx 0$ for the final state, so that the transition has negligible effect on the drive. Lastly, for $w=4.1$ (dashed-dotted line) the intermediate unforced roots have disappeared through merging and the island slows to the smallest root at $u \approx 0.15$. In this state the polarization current is stabilizing and the island quiescent.

In summary, we have described the interaction between magnetic islands and the electrostatic turbulence caused by dissipative drift waves. We used parity constraints to compare quiescent and turbulent states with the same values of the parameters. The most important effect of turbulence is to cause transitions to more slowly propagating states with partially flattened density. For a small island ($w=0.5$) the transition is destabilizing but for $w=2.9$ the effect on stability is very small and for large islands ($w=4.1$) it becomes stabilizing.

The authors acknowledge fruitful discussions with B. Breizman and M. Ottaviani. This work is funded by US DOE Contract No. DE-FG03-96ER-54346, and by the Center for Multiscale Plasma Dynamics under Contract No. DE-FC02-04ER54785.

- ¹J. Birn, *J. Geophys. Res., [Space Phys.]* **97**, 16817, DOI: 10.1029/92JA01527 (1992).
- ²Q. Chen, A. Otto, and L. C. Lee, *J. Geophys. Res.* **102**, 151, DOI: 10.1029/96JA03144 (1997).
- ³L. Ofman, P. J. Morrison, and R. S. Steinolfson, *Astrophys. J.* **417**, 748 (1993).
- ⁴R. Lahaye, *Phys. Plasmas* **13**, 056113 (2006).
- ⁵S. Inagaki, N. Tamura, K. Ida *et al.*, *Phys. Rev. Lett.* **92**, 055002 (2004).
- ⁶W. Horton, *Rev. Mod. Phys.* **71**, 735 (1999).
- ⁷B. D. Scott, H. Biglari, P. W. Terry, and P. H. Diamond, *Phys. Fluids B* **3**, 51 (1991).
- ⁸M. Ottaviani, F. Porcelli, and D. Grasso, *Phys. Rev. Lett.* **93**, 075001 (2004).
- ⁹J. D. Meiss, R. D. Hazeltine, P. H. Diamond, and S. M. Mahajan, *Phys. Fluids* **25**, 815 (1982).
- ¹⁰C. J. McDevitt and P. H. Diamond, *Phys. Plasmas* **13**, 032302 (2006).
- ¹¹A. Ishizawa and N. Nakajima, *Phys. Plasmas* **14**, 040702 (2007).
- ¹²A. Furuya, S. I. Itoh, and M. Yagi, *J. Phys. Soc. Jpn.* **70**, 407 (2001).
- ¹³A. Furuya, S. I. Itoh, and M. Yagi, *J. Phys. Soc. Jpn.* **71**, 1261 (2002).
- ¹⁴F. L. Waelbroeck, J. W. Connor, and H. R. Wilson, *Phys. Rev. Lett.* **87**, 215003 (2001).
- ¹⁵P. H. Rutherford, *Phys. Fluids* **16**, 1903 (1973).
- ¹⁶F. Militello and F. Porcelli, *Phys. Plasmas* **11**, L13 (2004); D. F. Escande and M. Ottaviani, *Phys. Lett. A* **323**, 278 (2004).
- ¹⁷A. Hasegawa and M. Wakatani, *Phys. Rev. Lett.* **50**, 682 (1983).
- ¹⁸A. I. Smolyakov, P. H. Diamond, and M. Malkov, *Phys. Rev. Lett.* **84**, 491 (2000).
- ¹⁹F. L. Waelbroeck, *Phys. Rev. Lett.* **95**, 035002 (2005).
- ²⁰C. Yu and D. Brower, *Nucl. Fusion* **32**, 1545 (1992).
- ²¹P. N. Guzdar, L. Chen, P. K. Kaw, and C. Oberman, *Phys. Rev. Lett.* **40**, 1566 (1978).
- ²²H. Sugama, M. Wakatani, and A. Hasegawa, *Phys. Fluids* **31**, 1601 (1988).
- ²³R. Fitzpatrick, F. L. Waelbroeck, and F. Militello, *Phys. Plasmas* **13**, 122507 (2006).